Effect of pressure on the elastic properties of vitreous As_2S_3

D. Gerlich,* E. Litov,† and O. L. Anderson
Institute of Geophysics and Planetary Physics, University of California, Los Angeles, California 90024
(Received 26 June 1978; revised manuscript received 23 April 1979)

The elastic properties of amorphous As_2S_3 have been measured as a function of hydrostatic pressure up to 20 kbar. The pressure dependence of the isothermal bulk modulus K_T is interpreted in terms of an interatomic potential, consisting of a Lennard-Jones and a Born-Mayer term. It is shown that this potential predicts a structural phase transition at a pressure range 350–400 kbar. A complete correlation is found to exist between the pressure dependence of the elastic properties and the pressure dependence of the rigid-layer modes as measured by Zallen on crystalline As_2S_3.

I. INTRODUCTION

The interest in chalcogenide glasses as photoconductors and their potential use as solid-state switches has stimulated intensive research into their optical and electrical properties. However, details of their disordered structure have proven to be more difficult to ascertain than their crystalline state. This is because x-rays and optical lines in the glassy state generally appear very broad and thus are less informative. Hence, different kinds of experiments are needed to reinforce any particular model proposed to account for the detailed structure.

High-pressure acoustic experiments are a useful tool in studying the nature of the bond forces in solids. These techniques have been recently applied to amorphous Se (a-Se) by Litov and Anderson[1] and to a-As_2Se_3 by Ota and Anderson.[2] The experiments involved the measurements of the velocities of shear and longitudinal sound waves as a function of hydrostatic pressure, up to ~20 kbar. The important quantity derived from these measurements is the isothermal bulk modulus K_T (inverse compressibility). Since K_T is related to the second derivative of the interatomic potential, it provides a sensitive test of the interatomic forces. The results on a-Se have shown that K_T can be derived from an interatomic potential which is dominated by a Lennard-Jones term at low pressures plus a Born-Mayer term at higher pressures. This appreciable deviation from a Lennard-Jones dependence at a relatively-low-pressure range was interpreted by Litov and Anderson[1] as being a percursor of the transition to metallic structure at the very-high-pressure range. Evidence that the chalcogenides, such as a-Se, a-As_2Se_3, and a-As_2S_3, undergo or tend toward a metallic transition at very high pressure was recently demonstrated by Minomura *et al.*[3] based on their electrical-conductivity measurements.

The microscopic mechanism leading to a metallic transition with pressure among the chalcogenides is understood in detail only in crystalline Se and Te.[4] In these cases, the application of hydrostatic pressure results in a denser packing of the chains and relatively little deformation along the stiff chains. This response is a manifestation of how pressure affects the electronic spatial distribution among the bonds in the chalcogenide groups. In Se, for example, with increasing pressure, charge is being promoted from the intrachain orbitals toward interchain orbitals. This increases the attractive interchain forces to the point that at a critical pressure these forces overcome the repelling Lennard-Jones forces, thus forcing the lattice to undergo a structural phase transition.

In this paper we describe high-pressure experiments on a-As_2S_3, similar to those performed on a-Se. Our results show that K_T has a similar pressure behavior to that in a-Se, thus reflecting the dominance of the weakly coupled layers on the compressibility. The fact that an additional term of the Born-Mayer type is needed to describe the interatomic forces indicates, just as in the case of a-Se, that with the application of pressure, charge is being redistributed from the intralayer to the interlayer regions, eventually causing at very high pressure a structural phase transition.

II. STRUCTURAL CONSIDERATIONS

Although the structure of As_2S_3 and As_2Se_3 is different from that of Se, they all possess common features that presumably will prove to have an important role in their behavior under very high pressure. Se has a one-dimensional chainlike structure in which the Se atoms are strongly bound to each other, whereas the interaction between the chains is much weaker and has been shown to be of the Van der Waals character. A similar picture is found in As_2S_3 and As_2Se_3. These two crystals possess a highly pro-

nounced layer structure,[5] with the layers stacking along the *b* direction. Within the layers, each As atom is threefold coordinated to form a pyramid structure, and each S atom is twofold coordinated, as can be seen in Fig. 1. This structure is also known as the orpiment structure. In the crystalline state the atoms in the layer are tightly bound in accordance with the covalent bonding requirements of atoms from columns 5 and 6 of the Periodic Table. The ratio between interlayer to intralayer bond length of $\sim$1.57 indicates that adjacent layers are held by a weak Van der Waals force. The layers can also be viewed as being made out of long As-S-As helical chains pointing along the *c* direction, with each chain coupled to its neighbors with a row of S atoms, or as interwoven puckered rings, each consisting of six pyramids.

The extent of disorder in the vitreous chalcogenides relative to the crystalline state is not known with certainty. This point was recently emphasized by Klein *et al.*,[6] who studied the Raman and infrared spectra of amorphous and crystalline As_2S_3. Their results on a-As_2S_3 indicate the presence of order beyond a single AsS_3 pyramid, but were insensitive to the details of the extended order. Thus, the structure of the layer still remains an open question, and at the present stage it is difficult to infer the existence of chains or layer segments in contrast to a random network of AsS_3 pyramids in the glassy state. Tsuchihashi and Kawamoto[7] also made comparative studies of amorphous and crystalline As_2S_3 using infrared and x-ray techniques. They attribute the lower density of a-As_2S_3 to an open structure in which the number of pyramids around the rings fluctuates between five and seven compared to the number of pyramids in the crystalline state, which is six.

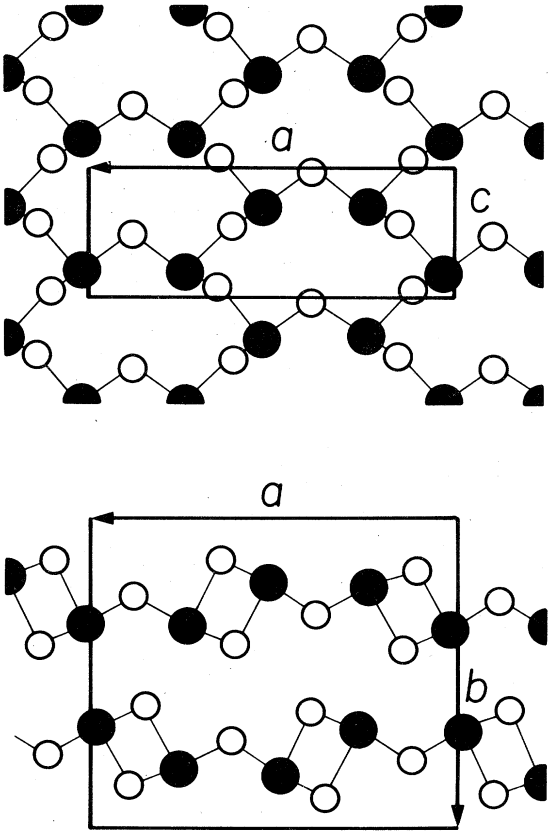

FIG. 1. Crystal structure of As_2S_3. The large dark circles are As atoms; small open circles are S atoms. The upper diagram is a projection along the [010] direction looking at the plane of the layers. The lower diagram is a projection along the [001] direction looking at the edges of the layer planes.

It is apparent from the orpiment structure of As_2S_3 that an application of moderate hydrostatic pressure to the crystalline material will result in a denser packing of the layers with little effect on the intralayer distances. The effect of pressure on packing in amorphous As_2S_3 will be more complex since in the glassy state loosely bound layer segments or chains can be affected with relative ease as adjacent layers.

III. EXPERIMENTAL

Cylinders of As_2S_3 glass, $\frac{1}{4}$ in. in diameter, were purchased from the Servo Corp. They were cut to size, and their end faces lapped flat and parallel. The elastic moduli were determined from the velocity and its pressure dependence for longitudinal and shear ultrasonic waves. The latter were generated by crystalline quartz transducers, *X* and *Y* cut, of 10-MHz frequency, bonded to the samples by a 1 : 1 formula weight mixture of glycerine and phthalic anhydride. Since the attenuation of the longitudinal wave was appreciable, the measurements of the pressure dependence of the velocity were performed here by the pulse-echo method, using unrectified echoes.[8] For shear waves, where the sound attenuation was much lower, the pulse superposition technique was used.[9] The absolute values of the elastic moduli were determined from the sound velocity measured by the pulse-echo technique.[8] The pressure was generated by means of a piston cylinder apparatus,[10,11] using a mixture of equal volumes of pentane and isopentane as the pressurizing fluid. A more detailed description of the cell experimental setup including the high-pressure cell is given in Refs. 1 and 11.

IV. RESULTS

Sound velocity in As_2S_3 glass exhibits some frequency dispersion.[12] Thus, in principle, all velocity values should be extrapolated to zero frequency be-

TABLE I. Zero-pressure, room-temperature elastic moduli and various other material parameters.

Quantity	Unit	Value
c_{11}^S	kbar	206.4
c_{44}	kbar	57.6
K^S	kbar	129.5
K_T	kbar	128.4
Density	g/cm^3	3.187
Constant pressure specific heat	J/(mole K)	120
Linear thermal expansion	α	2×10^{-5}

fore they can be used to evaluate the static elastic moduli. From the data of Ng and Sladek,[12] it is evident that this effect is quite small in the frequency range of 0–10 MHz. Since the velocity is proportional to the frequency, the change between 0 and 10 MHz will be about 1%. Thus, for all practical purposes, the use of 10-MHz data is justified.

The elastic constants from which the bulk modulus is calculated for a-As_2S_3 are C^l and C^t, where l is longitudinal waves and t is transverse waves. It is easy to show[1,13] that the elastic moduli, C_s^l, C_s^t, and K_s, corrected for variations in the sample path length l and density ρ, are given by

$$C_s^l = C_{0s}^l \left(\frac{f^l}{f_0^l}\right)^2 s \ , \tag{1a}$$

$$C_s^t = C_{0s}^t \left(\frac{f^t}{f_0^t}\right)^2 s \ , \tag{1b}$$

$$K_T = \frac{1}{1+\alpha\gamma T}\left(C_s^l - \tfrac{4}{3}C_s^t\right) = \kappa s \ , \tag{2a}$$

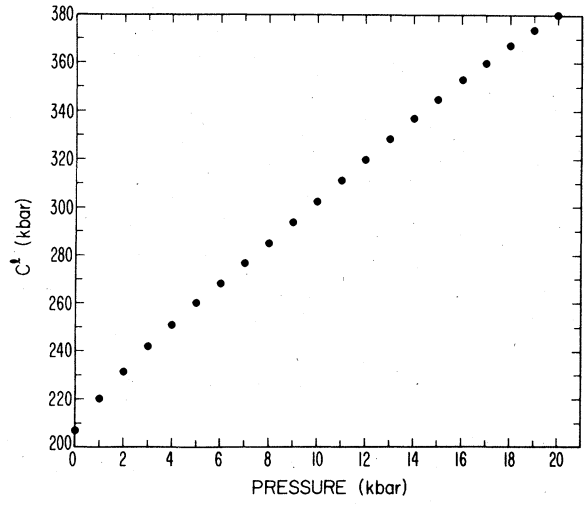

FIG. 2. Elastic constant C^l of a-As_2S_3 vs pressure.

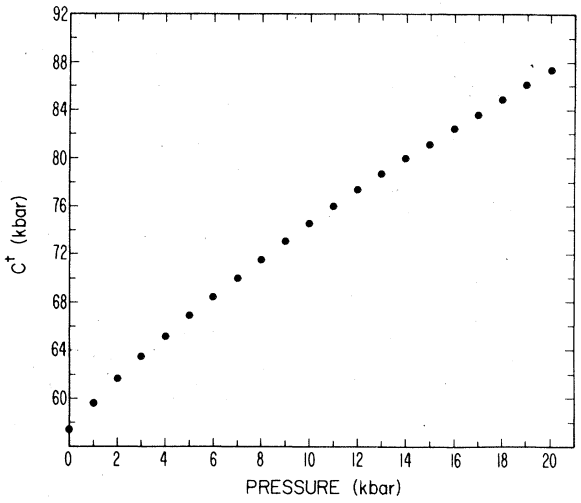

FIG. 3. Elastic constant C^t of a-As_2S_3 vs pressure.

where

$$\kappa = \left[C_{0s}^l \left(\frac{f^l}{f_0^l}\right)^2 - \tfrac{4}{3}C_{0s}^t \left(\frac{f^t}{f_0^t}\right)^2\right]\frac{1}{1+\alpha\gamma T} \tag{2b}$$

and

$$s = 1 + \tfrac{1}{3}\int_0^p \frac{dp}{\kappa} \tag{3}$$

and where f is the frequency, α the coefficient of expansion, γ the Grüneisen constant, p the pressure, T the temperature, and $s = l_0/l$ for isotropic solids is a measure of the sample's compression. The small correction $\alpha\gamma T = 0.001$ in Eq. (2) was assumed to be independent of pressure. The zero subscripts refer to 1-bar values of the various quantities.

In Eq. (2b) κ is a measurable quantity and its sub-

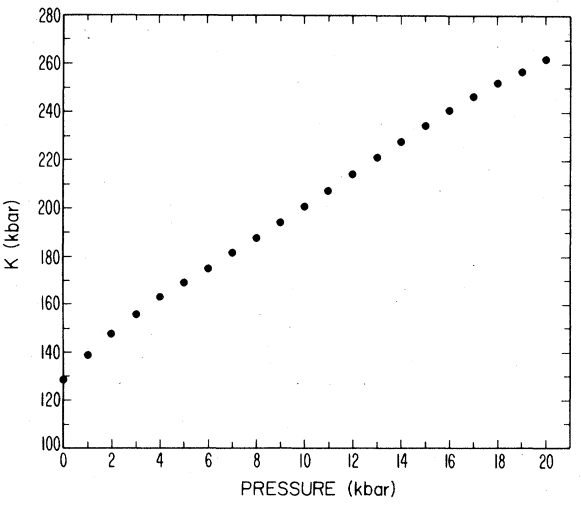

FIG. 4. Bulk modulus K_T of a-As_2S_3 vs pressure.

TABLE II. Isothermal bulk modulus and compression as a function of pressure.

P (kbar)	K_T (kbar)	V/V_0
0	128.8	1.0000
1	139.5	0.9926
2	148.3	0.9857
3	156.0	0.9792
4	163.0	0.9731
5	169.4	0.9673
6	175.7	0.9617
7	181.9	0.9563
8	188.2	0.9512
9	194.6	0.9462
10	201.2	0.9414
11	208.0	0.9368
12	214.8	0.9324
13	221.6	0.9282
14	228.3	0.9241
15	234.8	0.9201
16	241.0	0.9162
17	246.8	0.9125
18	252.2	0.9088
19	257.2	0.9053
20	261.8	0.9018

stitution in Eq. (3) leads to the evaluation of s. Table I presents the measured values of the room-temperature adiabatic elastic moduli, together with other pertinent material parameters used in the above calculations. The results for C^l, C^t, and K_T are shown in Figs. 2, 3, and 4, respectively. In Table II the pressure dependence of K_T and the compression $v = V/V_0 = 1/s^3$ are presented in numerical values.

In Table III we show the pressure derivatives of the elastic moduli at zero pressure. It is noted that $K_T'(0) \simeq 7.5$, which is high by comparison to "normal" solids ranging around 4. Values of $K_T'(0) \sim 8$ were also found for a-Se,[1] a-As_2Se_2 indicating, as we shall discuss later, that the interatomic forces in these materials are similar.

V. DISCUSSION

A. Interatomic potential

The fact that the interlayer atomic separation in a-As_2S_3 varies between 3.56 and 5.00 Å led Zallen *et al.*[14] to assume, on the basis of the Pauling criteria, that the major interlayer forces must have the characteristics of Van der Waals forces. Similar arguments were used to derive the nature of other interchain forces on a-Se.[15] However, when both materials are subjected to increased hydrostatic pressure, the elastic data reveal appreciable deviation from a Van der Waals dependence. In a-Se this deviation was recognized because of the effect of pressure on the charge spatial distribution between intrachain and interchain regions.[4] This has the effect of increasing the attracting interchain forces and thus lowering the total energy. Ample evidence for these effects were provided by optical experiments on a-Se in which intrachain modes decrease and interchain modes increase with pressure.[16] Theoretical calculations by Joannopoulos, Schlüter, and Cohen[17] have also supported these conclusions. It appears that similar effects take place in the two-dimensional chalcogenides As_2S_3 and As_2Se_3. In both cases, the chalcogen atom enters into a covalent bonding with a pair of its two nearest neighbors, using two of the six s^2p^4 valence electrons, while the other four form two lone-pair orbitals that protrude into the intermolecular regions. In Se, under the effect of very high pressure, these orbitals strongly overlap to form a covalent bonding as manifested by the transition to the metallic state.[3] The evidence, based on electric conductivity measurements of Minomura *et al.*,[3] is that a-As_2S_3 and a-As_2Se_4 will also transform to the metallic state at pressures greater than ~300 kbar. Evidence for charge promotion from the intralayer to the interlayer regions is derived from pressure-optical experiments on these materials by Zallen *et al.*[14] Here too it is observed that two of the intralayer modes decrease with increased pressure, whereas all the interlayer modes increase with pressure. In the following, we will demonstrate that the elastic properties in a-As_2S_3

TABLE III. Pressure derivatives of the elastic moduli.

	$\frac{\partial c_{11}}{\partial P}$	$\frac{\partial c_{44}}{\partial P}$	$\frac{\partial K}{\partial P}$	$\frac{\partial^2 c_{11}}{\partial P^2}$ (kbar^{-1})	$\frac{\partial^2 c_{44}}{\partial P^2}$ (kbar^{-1})	$\frac{\partial^2 K}{\partial P^2}$ (kbar^{-1})
Adiabatic	10.0 ± 0.4	1.91 ± 0.035	7.51 ± 0.45	−0.16 ± 0.017	−0.050 ± 0.002	−0.100 ± 0.014
Isothermal			7.51 ± 0.45			−0.099 ± 0.014

can also be treated on the basis of the above microscopic picture.

As mentioned before, the Van der Waals potential was found to be inadequate for describing the elastic properties as a function of pressure. In particular, the experimental values of K_T as evaluated from the elastic constants plotted in Fig. 3 were found to deviate appreciably below the K_T as derived solely from the Van der Waals potential. The agreement can be improved by taking into account the extra interaction term, originating from the lone-pair orbitals overlapping with antibonding states at different layers. Since the interlayer distances are on the order of 4–5 Å, it is reasonable to assume, just as we did for Se, that the wave-function spatial dependence along other lone-pair direction is asymptotically exponential. Adding this term to the Lennard-Jones potential, the total interatomic potential takes the following form:

$$\phi(\bar{R}) = A/\bar{R}^m - B/\bar{R}^n - Ce^{-\lambda\bar{R}} \ , \tag{4}$$

where A, B, C, and λ are constants and $\bar{R}$ is the average interlayer distance. In Eq. (4) we have assumed that $\phi(\bar{R})$ is simply a function of $\bar{R}$ excluding any dependence on the intralayer distance r. Later on it will be seen that these assumptions are adequate, since the contribution to compression by the internal covalent bonds is negligible in comparison with the contribution by the interlayer bonds. A very important feature of $\phi(\bar{R})$ is that its third term is responsible for a structural phase transformation at very high pressures. At some critical pressure P_c, its attractive character overcomes the repelling $1/\bar{R}^{12}$ term, thus destabilizing the structure and forcing it into another phase. These features, as we shall see below, will allow us to predict a phase transformation in a-As_2S_3 at pressures well above 350 kbar. This is done by analyzing K_T as derived from $\phi(\bar{R})$ in terms of our present experimental data. Using the well-known definition for the bulk modulus

$$K_T = V\frac{\partial^2\phi}{\partial V^2} \tag{5}$$

we obtain, using Eq. (4),

$$K_T = a\,[180x^5 - 54x^3 + (6-12B)x^{1/3} \times (2x^{1/3}+\lambda)e^{\lambda(1-x^{-1/3})}] \ , \tag{6}$$

where $a = A/9V_0$, x is the reduced density, C is eliminated by the equilibrium condition, and B is evaluated by requiring K_T to become zero at the transition density x_C. After a few manipulations one obtains

$$B = \frac{9x_c^3 - F(x_c;\lambda)}{2[15x_c^5 - F(x_c;\lambda)]} \ , \tag{7}$$

where

$$F(x_c;\lambda) = x_c^{1/3}(2x_c^{1/3}+\lambda)e^{\lambda(1-x_c^{-1/3})} \tag{8}$$

These constraints leave Eq. (6) with only a normalizing contant a and two fitting parameters λ and x_c. However, as we shall see, the critical normalized density x_c is constrained to values of 1.65 to 1.85, thus, basically, leaving Eq. (6) with only one fitting parameter λ.

In deriving Eq. (6) it was assumed that for the amorphous state the volume contracts as $V \sim \bar{R}^3$. It should be noted that for the crystalline state, in which the layers are neatly stacked, $V \simeq A\bar{R}$, where A is the cross-sectional area of the layer planes, and which under moderate pressure remains constant. The above difference for the functional dependence of V on $\bar{R}$ for the amorphous case arises, because in this state the infinite layer planes are broken into very small segments, whose size are on the order of a few Angstrom long, and are randomly oriented with respect to each other. Under these conditions, the volume, under the effect of hydrostatic pressure, will decrease isotropically. Assuming that only interlayer motion is allowed it is clear that each dimension of the macroscopic sample will contract as $\sim\bar{R}$ and thus, the volume will contract as $V \sim \bar{R}^3$. The fact that the density of the vitreous As_2S_3 is smaller than that of the crystalline As_2S_3 indicates that voids are present among the broken-layer segments. Their volume-pressure relationship is probably also dictated by Van der Waals forces, such as described by Eq. (4), and their volume will contract under the effect of pressure as l^3, where l is an effective size of the voids. The effective interlayer distance $\bar{R}$, then, includes also the effect of voids.

Equation (6) for K_T was fitted to our data and the results are shown in Fig. 5. The best fit was achieved with parameters $a = 3.72$, $\lambda = 38$, $x_c = 1.75$, and B

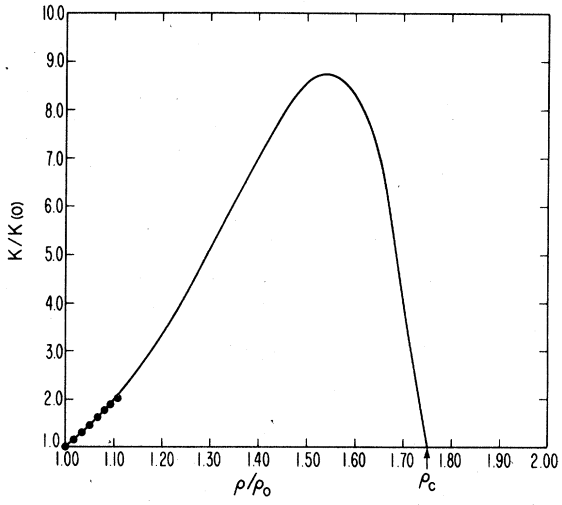

FIG. 5. Bulk modulus K_T of a-As_2S_3 vs ρ/ρ_0. Solid curve is due to Eq. (6). Arrow indicates the density at which phase transition is predicted.

derived from Eq. (7) is 0.5032. As can be seen, the fit is reasonably good. The value of normalized density $x_c = 1.75$ corresponds to a predicted critical pressure of about 350–400 kbar. The predictions can be tested experimentally since this range of pressure is accessible through the apparatus of the diamond anvils. Unfortunately, Minomura *et al.*[3] did not carry their electrical measurements on a-As_2S_4 and a-As_2Se_3 beyond 250 kbar. Their results show that in both materials, the electrical resistivity decreases very sharply with pressure, and around 250 kbar attains metallic characteristics. Hence if our assumption is correct that $\phi(\bar{R})$ in Eq. (4) does indeed characterize the major interatomic forces, then it is anticipated that a-As_2S_3 will exhibit a phase transformation at around 350–400 kbar.

B. Comparison with the optical data

We will now examine the extent to which our elastic data and the interatomic potential $\phi(\bar{R})$ correlate with the available optical Raman data. Several optical Raman experiments on vitreous and crystalline As_2S_3 have been carried out, both as a function of temperature and pressure.[6,7,18,19] Kobliska and Solin,[19] who compared the Raman spectra of As_2S_3 in the crystalline state with that in the vitreous state, were able to provide valuable information about the vibrational and structural properties of both. The optical data tend to support a picture in which both the layer characters as well as the pyramid units are well preserved in the vitreous state. This is particularly reflected in the optical spectra of the two phases when a comparison of the density of vibrational states of amorphous and cyrstalline As_2S_3 is made. Kobliska and Solin find that the two data sets are remarkably similar in the sense that the density of states for the vitreous phase is basically the envelope of the corresponding crystal-data points. Furthermore, they showed that the continuous Raman spectra of vitreous As_2S_3 [including the rigid-layer (RL) modes region] could be easily accounted for by assuming a slight distribution in both force constants of the fundamental modes and the pyramid apex angles. The fact that the intermolecular forces retain their basic identity in vitreous As_2S_3 allows us to compare our elastic data in a-As_2S_3 with optical data of the crystalline state.

We make the comparison with the optical data assuming, as before, that under moderate hydrostatic pressure the elastic properties in vitreous As_2S_3, to first order, will be affected only by the interlayer forces. It is very easy to show[20] that for a one-dimensional chain the force constant k is related to the elastic stiffness constant c of the line by the relation $c = ka$, where a is the interatomic separation. For a three-dimensional structure, a similar relation can be derived, using a simple dimensional argument; i.e., that there are $\sim 1/a^2$ chains per unit area. This gives a force constant that is related to the elastic constant as

$$k = ac \quad . \tag{9}$$

Hence, there should be an intimate relationship between the elastic constants c_{11} and c_{44} and the rigid-layer compressional and shear mode force constants, respectively. Several years ago, Zallen[18] measured the Raman spectra of crystalline As_2S_3 as a function of pressure up to 10 kbar. From his results he was able to identify the rigid-layer modes and study their pressure dependence. At zero pressure he finds that the compressional spring constant is $k_i^{\text{comp}} = 9 \times 10^2$ N/m and that the two nondegenerate shear constants are $k_i^{\text{shear}} = 1.8 \times 10^2$ N/m and $k_i^{\text{shear}} = 3.5 \times 10^2$ N/m. Viewing a-As_2S_3 as an effective three-dimensional interlayer network of chains with effective interlayer distance $\bar{R}_0$, we can use Eq. (9) to estimate the RL spring constants. Substituting our values of c_{11} and c_{44}, and taking the average reported interlayer distance as $\bar{R}_0 = 4.5$ Å, we get $k_i^{\text{comp}} = 9 \times 10^2$ N/m and $k_i^{\text{shear}} = 2.6 \times 10^2$ N/m. The latter value for k_i^{shear} is exactly the average value of the two nondegenerate shear mode spring constants, as reported above by Zallen. This excellent agreement between our estimated force constants and the rigid-layer spring constants indicates that the elastic properties are primarily dominated by the interlayer forces. Additional support for that notion comes from the pressure dependence of the effective spring constant evaluated from the interatomic potential $\phi(\bar{R})$. As noted before, [Eq. (6)], the bulk modulus K_T as evaluated from $\phi(\bar{R})$ agrees well with our experimental results. This indicates, in view of our conclusions above, that the pressure dependence of the effective spring constant, defined as $k_i^{\text{eff}} \equiv \partial^2\phi(\bar{R})/\partial^2\bar{R}$, should reflect the pressure dependence of those reported by Zallen for the crystalline As_2S_3. Taking the second derivative of Eq. (4) with respect to $\bar{R}$, we get

$$K_i^{\text{eff}} = A\left[\frac{m(m+1)b}{\bar{R}^2}\left(\frac{\bar{R}_0}{\bar{R}}\right)^m - \frac{n(n+1)}{\bar{R}^2}\left(\frac{\bar{R}_0}{\bar{R}}\right)^n + \frac{\lambda(n-mb)e^{\lambda}}{(\bar{R}_0)^2}e^{-\lambda(\bar{R}/R_0)}\right] . \tag{10a}$$

Substituting the values for $m = 12$, $n = 6$, $\lambda = 38$, $b = 0.5032$, and $v = (\bar{R}/\bar{R}_0)^3$, we get

$$K_i^{\text{eff}} = \frac{A}{\bar{R}_0^2}\left[78.4\left(\frac{1}{v}\right)^{14/3} - 42\left(\frac{1}{v}\right)^{8/3} - (4.648 \times 10^{16})e^{-38v^{1/3}}\right] . \tag{10b}$$

$k_i^{\text{eff}}/k_i^{\text{eff}}(0)$, where $k_i^{\text{eff}}(0)$ is the zero-pressure value of k_i^{eff}, may now be evaluated as a function of the pressure, and the results are plotted in Fig. 6 along with the normalized rigid-layer spring constants associated with the 25, 36, 62, and 69 cm^{-1} modes. We see that the k_i^{eff} rate of increase with pressure is about the average of all the RL modes. This is reasonable in view of the average properties of $\phi(\bar{R})$. However, a more plausible explanation can be given by evaluating the effective macroscopic compressibility β from RL force constants k_i. This can be performed using Zallen's scaling force law for molecular crystals.[18] From his pressure (Raman) experiments on S_8 and As_2S_3, Zallen finds that the Grüneisen parameter $\gamma_i = (1/\beta)(d \ln \nu_i/dP)$ for the phonon i, where ν_i is the frequency, is very much frequency dependent, falling sharply from values of order 1 at low frequencies to values of order 10^{-2} at high frequencies. This, as it is well known, is inconsistent with the usual frequency Grüneisen scaling law for regular three-dimensional network crystals. In his model, Zallen assumed that the bond force constant/bond strain relation for each bond type i continues to obey the scaling law

$$k_i(\xi_i) \sim \xi_i^{-6\gamma} \ , \tag{11a}$$

where $\gamma \simeq 1$, ξ_i is the microscopic strain, and the γ_i are assumed to obey the scaling relation

$$k_i(\eta) \sim \eta^{-6\gamma_i} \ , \tag{11b}$$

where now η is the macroscopic strain $\eta = \sum_i \xi_i$. He then proceeds to show that the γ_i rougly scale according to

$$\gamma_i = 2\left[\frac{k_1}{k_i}\right]\gamma \ , \tag{12}$$

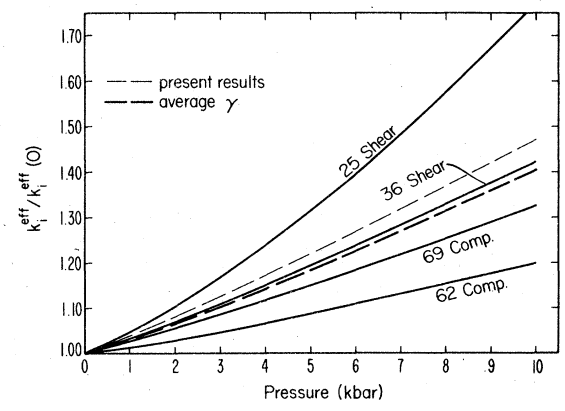

FIG. 6. Rigid-layer modes force constants of crystalline As_2S_3 vs pressure. Superimposed is K^{eff} derived from $\phi(\bar{R})$ [data after Zallen (Ref. 18)].

TABLE IV. Rigid-layer modes and their associated γ's, calculated from Eq. (11b).

Mode (cm^{-1})	γ
25	4.60
36	2.82
62	1.39
69	2.27
average	2.77

where k_1 is the force constant for the lowest mode. Since $\nu_i \sim k_1^{1/2}$ and from Eq. (12), $\gamma_i \sim \nu^{-2}$, as experimentally observed by Zallen. Equation (11a) basically states that with increased pressure, all force constants obey a "universal" law with respect to their microscopic strain, whereas according to Eqs. (11b) and (12), they differ with respect to the macroscopic strain. It is clear that softer bonds will have γ_i larger than the harder ones, since under hydrostatic pressure most of the volume change is soaked up by the softer bonds. From Eqs. (11b) and (12), it is now also clear why the force constant of the lower modes rises faster with pressure than the upper modes.

Now, in order to account for our pressure dependence of the effective force constant k_i^{eff}, shown in Fig. 6, we apply Zallen's model. Using similar arguments, it can be easily shown using Eq. (11) that the Grüneisen parameter γ_i scale according to

$$\gamma_i = \gamma \frac{\beta_i}{\beta} \ , \tag{13}$$

where β_i is the individual bond-type i compressibility. From Eq. (11b), we see that γ_i controls the rate of increase of each force constant. It is clear then, from Eq. (13), that an effective γ^{eff} which corresponds to k_i^{eff} could be evaluated if a procedure for evaluating β^{eff} were known. Such a task for vitreous As_2S_3 is obviously too formidable at the present time. However, in searching for an averaging procedure, we have found that a simple mathematical average of γ_i (excluding any internal vibrations) gives a very good fit to our data (Fig. 6). This implies through Eq. (13) that β^{eff} is just a mathematical average of the individual β_i, i.e., $\beta^{\text{eff}} = (1/n)\sum_i^n \beta_i$. It is interesting to note that for composite materials such as rocks with disparate compressibilities, mathematical average seems to give reasonable results.[21] In Table IV, we list those γ_i used in the above calculations. We see that $\gamma^{\text{eff}} = 2.77$ compared to an experimental value of 3.1.

VI. CONCLUSIONS

Measurements of the elastic moduli of a-As_2S_3 up to 20-kbar pressure are reported. The bulk modulus evaluated from the above data is interpreted in terms of an interatomic potential, consisting of a Lennard-Jones term and a Born-Mayer term. The inclusion of the Born-Mayer term is based on the microscopic structure of a-As_2S_3 and the variation in its electronic spatial distribution as a function of pressure. The above potential predicts a phase transformation at a pressure of 350–400 kbar, a fact which is borne out by the electrical measurements. A comparison of the acoustic and optical data reveals a complete correlation between the pressure dependence of the elastic properties and the behavior of a rigid-layer model under pressure.

ACKNOWLEDGMENTS

The authors wish to express their gratitude to Professor George C. Kennedy for his generous support of the project and to Dr. R. Boehler for his assistance in the high-pressure cell design. One of us (E.L.) wishes to thank Dr. R. Zallen for a number of helpful discussions. This research was partly supported by NSF Grant No. DMR 76-18740. Publication #1829, Institute of Geophysics and Planetary Physics, University of California, Los Angeles.

---

*On sabbatical leave from the Dept. of Phys. and Astron., Tel Aviv Univ., Ramat Aviv, Israel.

†Permanent address: R&D Associates, 4640 Admiraly Way, Marina del Rey, Calif. 90291.

[1]E. Litov and O. L. Anderson, Phys. Rev. B 18, 5705 (1978).

[2]R. Ota and O. L. Anderson, J. Non-Cryst. Solids 24, 235 (1977).

[3]S. Momura, K. Aoki, and O. Shimonura, in *Proceedings of the Sixth International Conference on Amorphous and Liquid Semiconductors, Leningrad, USSR, 1975* (Nauka, Leningrad, 1976), p. 18.

[4]R. M. Martin, G. Luckovsky, and K. Hellwell, Phys. Rev. B 13, 1383 (1976).

[5]N. Morimoto, Mineral J. (Sapporo) 1, 160 (1954).

[6]P. B. Klein, P. C. Taylor, and D. J. Treacy, Phys. Rev. B 16, 4511 (1977).

[7]Shoj Tsuchihashi and Yoji Kawamoto, J. Non-Cryst. Solid 5, 286 (1971).

[8]H. J. McSkimin, J. Acoust. Soc. Am. 33, 12 (1961); 34, 609 (1962); 37, 864 (1965); 43, 864 (1968).

[9]E. Litov, Rev. Sci. Instrum. 47, 880 (1976).

[10]J. C. Haygarth, I. C. Getting, and G. C. Kennedy, J. Appl. Phys. 38, 4557 (1967).

[11]R. Boehler, I. C. Getting, and G. C. Kennedy, J. Phys. Chem. Solids 38, 233 (1977).

[12]D. Ng and R. J. Sladek, Phys. Rev. B 11, 4017 (1975).

[13]R. K. Cook, J. Acoust. Soc. Am. 29, 445 (1957).

[14]R. Zallen, M. L. Slade, and A. T. Ward, Phys. Rev. B 12, 4257 (1971).

[15]K. Vedam, D. L. Miller, and R. Roy, J. Appl. Phys. 37, 3432 (1966).

[16]W. Richter, J. B. Rinucci, and M. Cardona, Phys. Status Solidi B 56, 223 (1973).

[17]D. J. Joannopoulus, M. Schlüter, and M. L. Cohen, Phys. Rev. B 11, 2186 (1975).

[18]R. Zallen, Phys. Rev. B 9, 4485 (1974).

[19]R. J. Kobliska and S. A. Solin, Phys. Rev. B 8, 756 (1973).

[20]C. Kittel, *Introduction to Solid State Physics,* 2nd ed. (Wiley, New York, 1956), Chap. 5.

[21]N. Warren (private communcation).